GEOCHEMICAL BEHAVIOUR OF RARE EARTH ELEMENTS (REE) ALONG A RIVER REACH RECEIVING INPUTS OF ACID MINE DRAINAGE

Manuel Olías[a,b,*], Carlos R. Cánovas[a,b], María Dolores Basallote[a,b] and Alba Lozano[c]

[a] Department of Earth Sciences, Faculty of Experimental Sciences, University of Huelva, Campus 'El Carmen' s/n, 21071 Huelva, Spain.

[b] Research Center on Natural Resources, Health and the Environment (RENSMA), University of Huelva, 8 21071 Huelva, Spain.

[c] Institute of Environmental Assessment and Water Research, CSIC, Jordi Girona 18, 08034 Barcelona, Spain.

* Corresponding author: Manuel Olías (manuel.olias@dgyp.uhu.es)

ABSTRACT

Total and dissolved rare earth elements (REE) were studied in a river reach affected by several inputs of acid mine drainage. The first four acidic discharges were of lesser importance compared to the last (Agrio River, coming from the Río Tinto mines), which transported high loads of Fe and Al (2.1 and 4.2 ton/day, respectively) together with REE (16.4 kg/day) and other trace elements. In the acid mine drainage (AMD) sources, practically all the REE were dissolved and the North American Shale Composite (NASC)-normalized patterns showed an enrichment in medium REE, although some differences exist between the patterns of each source. The pH values in the river reach upstream of the confluence with the Agrio River ranged between 8.01 to 7.03, and most of the Fe and Al from the AMD sources precipitated. Downstream of this acidic discharge, the pH decreased to 2.98. Upstream of the first AMD input, the dissolved and total concentrations of ΣREE were very low (< 0.6 μg/L). In the river reach affected by AMD that maintains pH values > 7, concentrations of ΣREE increased (up to 25 μg/L), mainly transported by the particulate phase. In the reach downstream of the Agrio River with acidic conditions, REE behaved conservatively. The REE NASC-normalized patterns of the river samples resemble that of the AMD sources, although an enrichment of heavy REE in the dissolved phase is observed linked to complexation by carbonates. Cerium and particularly La also show higher dissolved percentages, similar to HREE, which must be due to the lower affinity of these elements to be sorbed onto Fe oxyhydroxides. Variations in Ce and Eu anomalies are observed along the river reach as a consequence of the different AMD inputs. However, the values of the Ce anomaly are higher in total samples than in dissolved samples. Speciation results indicate that these differences are not caused by differences in oxidation states but by slight differences in the hydrogeochemical behaviour of Ce with respect to La and Nd.

Key words: Rare earth partitioning, acid mine drainage, Iberian Pyrite Belt

1. INTRODUCTION

Rare earth elements (REE) are a group of chemically similar metallic elements, from La to Lu. However, as long as their atomic number increases, a decrease in their ionic radii is observed. This process, known as lanthanide contraction, is the main one responsible for the subtle geochemical differences among REE (Migaszewski and Galuszka, 2015). All REE occur in a trivalent state in nature except for Ce and Eu, which can have a valence of +4 and +2, respectively, exhibiting different behaviour under changing redox conditions.

Due to their particular properties, REE have been widely used to infer petrogenetic processes. More recently, REE have been profusely used as tracers to unravel hydrogeochemical processes (e.g., Johannesson et al., 1997; Dia et al., 2000; Worral and Pearson, 2001; Pérez-López et al., 2015). In addition, their similarity to trivalent actinides has allowed the prediction of the behaviour of these elements in nature (e.g., Verplanck et al., 1999; Stille et al., 2003). On the other hand, REE have become increasingly important in the technological industry, mainly for the production of electronic devices; thus, REE demand has exploded worldwide in the last decade (Hatch, 2012; Migaszewski and Galuszka, 2015). Along with the recent rise in use, there is a growing concern about the impact of the release of REE on the environment and human health such that REE are currently considered as emerging pollutants (Kulaksiz and Bau, 2007; Migaszewski and Galuszka, 2015; Huang et al. 2016; Kurvet et al., 2017).

The high concentrations of REE in acidic mine drainage (AMD) generated during sulphide and coal mining have also attracted great interest in the study of 1) water–rock interaction processes (e.g., Ferreira da Silva et al., 2009; Grawunder et al., 2014), 2) the natural or anthropogenic origin of acidic drainage (e.g., Verplanck et al., 1999), and 3) the potential recovery of REE from acidic mine waters (e.g., Ayora et al., 2016; Nordstrom et al., 2017). However, the toxicity and geochemical behaviour of REE in circumneutral waters receiving inputs of AMD (Verplanck et al., 2004; Gammons et al., 2005) has attracted less attention, as opposed to other elements commonly found at higher concentrations and/or of greater toxicity such as As, Pb, or Cd (e.g., Sarmiento et al., 2009; Nieto et al., 2013). Thus, the main goal of this work is to study the geochemical behaviour of REE (dissolved and particulate) along a river reach affected by several REE-rich AMD inputs that is characterized by a progressive change from alkaline pH values to acidic conditions (pH < 3).

2. SITE DESCRIPTION

The study reach (8 km in length) comprises the upper part of the Odiel River (Fig. 1). The river runs through rhyolite and dacite rocks belonging to the Volcano-Sedimentary Complex of the Iberian Pyrite Belt (IPB), which contains massive sulphide deposits, and shales from the Culm Group (Sáez et al., 1999). Pyrite is the main component of the sulphide deposits (> 90%), although minor

quantities of chalcopyrite, sphalerite, galena, and other accessory minerals are found (Tornos, 2006).

The climate of the study area is Mediterranean in type characterized by mild winters and hot summers, with an average temperature of 16.5°C. The annual average precipitation in the area is around 750 mm, mainly collected during autumn and winter. River flows in winter usually range from 1 to 3 m^3/s, decreasing progressively during spring and summer (Cánovas et al., 2018). However, due to the low permeability of the basin materials, the occurrence of intense rainfall may cause flood events, strongly increasing river flow (Galván et al., 2016).

There are four relatively small derelict mines located in the study area (Fig. 1). Concepcion mine was intensively exploited from 1852 to 1990, with a total sulphide production of around 2 Mt. Mining activities in San Platón (from 1907 to 1934), Esperanza (from 1906 to 1931), and Poderosa (from 1864 to 1924) ceased earlier, and sulphide production was of minor importance (Pinedo Vara, 1963). Several permanent AMD discharges arise from these derelict mines. A passive treatment plant based on the Dispersed Alkaline Substrate (DAS) technology has been built at the Esperanza mine (Fig. 1), but some acidic discharges still occur (Cánovas et al., 2018). The surroundings of these mines are covered by spoil heaps (Fig. 1), which also constitute a diffuse source of dissolved and particulate metals entering the river during rainfall events.

Acidic leachates from the huge Río Tinto mines, which were intensively exploited from 1873 to 2000 (Olías and Nieto, 2015), are collected by the Agrio River, which joins the Odiel River just at the end of the reach (Fig. 1). The Agrio River causes strong degradation of the Odiel River water quality (Sánchez España et al., 2006; Cánovas et al., 2018).

3. METHODOLOGY

Sampling was performed in the study reach of the Odiel River during November of 2016. The main AMD inputs into the river were sampled (points CON, SPL, ESP, POD, and AGR; Fig. 1) as well as the river itself upstream and downstream of the confluence of each AMD source (points O1 to O8; Fig. 1). Samples were collected in HDPE bottles previously washed with a solution of 10% HNO_3, prepared with Nitric Acid 65% Merck Suprapur®. Total (raw) and filtered samples (0.2 µm pore size) were collected, acidified to pH < 2 with Nitric Acid 65% Merck Suprapur®, and refrigerated until Inductively Coupled Plasma-Atomic Emission Spectroscopy (ICP-AES) and Inductively Coupled Plasma-Mass Spectroscopy (ICP-MS) analysis. The particulate fraction was estimated from the difference in values between the raw and filtered samples.

Temperature, pH, electrical conductivity (EC), and oxidation-reduction potential (ORP) were measured in situ using a Crison MM40+ multimeter. A three-point calibration was performed for both EC and pH (147 µS/cm, 1413 µS/cm, and 12.88 mS/cm and 4.01, 7.00, and 9.21, respectively), while ORP was controlled using two points (240 and 470 mV). ORP measurements were corrected to the standard hydrogen electrode to calculate pE (Nordstrom and Wilde, 1998). The alkalinity was determined using volumetric titration test kits (HI3811). Flows were measured using an

electromagnetic flowmeter. Some discharge data were also obtained by a mass balance approach using the MIX code, a maximum likelihood method to estimate mixing ratios, while acknowledging the uncertainty in end-member concentrations (Carrera et al., 2004).

Samples were analysed by ICP-AES (Jobin Yvon Ultima 2) for major cations and ion chromatography (Dionex DX-120) for Br^-, Cl^-, F^-, NO_3^-, NO_2^-, PO_4^{3-}, and SO_4^{2-} at the R+D laboratories of the University of Huelva and by triple-quadrupole ICP-MS (iCAP TQ ICP-MS; ThermoFisher Scientific) for trace elements at Actlabs Ltd (Ontario, Canada). Detection limits ranged from 10 to 0.2 µg/L for the main elements (e.g., Al, Ca, Fe, Mg, Na, K, and Si) analysed by ICP-AES and from 0.0009 to 0.3 µg/L for elements analysed by ICP-MS (Supplementary Material SM2). The detection limit for REE ranged from 0.001 µg/L for La, Ce, Nd, Sm, Gd, and Dy to 0.0003 µg/L for Er (Supplementary Material SM3). A certified reference material (IV-STOCK-1643 by Inorganic Ventures) was analysed to check for accuracy. Differences between certified and measured values ranged from -1.8% to 10% (interquartile range). Precision was evaluated by analysing duplicates, and differences among values were below 1%.

In this paper, La through Sm are considered light rare earth elements (LREE), Eu through Dy middle rare earths (MREE), and Ho to Lu heavy rare earths (HREE). In order to study fractionation processes during the mixing of AMD sources and the river water, REE concentrations were normalized using the North-American Shale Composite (NASC) values (Taylor and McLennan, 1985). Cerium (Ce*) and Europium (Eu*) anomalies were calculated from the expression $Ce_{NASC}/\sqrt{[La_{NASC}\cdot Pr_{NASC}]}$ and $Eu_{NASC}/\sqrt{[Sm_{NASC}\cdot Gd_{NASC}]}$, respectively (Taylor and McLennan, 1985; Worrall and Pearson, 2001). NASC-normalized REE signatures were described using the NASC-normalized ratios, $(MREE/LREE)_N$ and $(HREE/MREE)_N$, calculated as the average of all permutations of these inter-element ratios (Stolpe et al., 2013). The LREE included in the ratio calculation were La, Pr, Nd, and Sm; the MREE were Gd, Tb, and Dy, and the HREE were Ho, Er, Tm, Yb, and Lu. Both Ce and Eu were excluded from the calculation due to their anomalous redox activity (Stolpe et al., 2013).

Chemical speciation was also obtained using the CHEAQS program version 2017.3 (Verweij, 2017). The CHEAQS model includes inorganic speciation and mineral equilibrium based on the National Institute of Standards and Technology database version 8.0 (NIST, 2004).

4. RESULTS

4.1. Characterization of the main AMD sources

The first four AMD discharges into the Odiel River (Fig. 1) show low flows (from 0.3 L/s in San Platón to 4.2 L/s in Concepción) whereas the flow carried by the Agrio River was noticeably higher (41 L/s; Supplementary Material SM1). The pH values of the main AMD sources show a slight variation, from 2.4 to 2.7. Dissolved and total concentrations are quite similar (Supplementary Material SM2 and SM3), with the highest values detected in the Agrio River (17.7 g/L sulphate,

1640 mg/L Mg, 1170 mg/L Al, 223 mg/L Zn, and so on), except for Fe and As which were observed to have their highest values in San Platón (1590 and 1.4 mg/L, respectively). Each of the first four AMD sources released Fe and Al loads between 5 and 50 kg/day to the river (Fig. 2) while those delivered by the Agrio River were notably higher (2.2 and 4.1 ton/day of Fe and Al, respectively).

Regarding the concentrations of ΣREE, the highest values were observed in the Agrio River, San Platón, and Poderosa (from 2.8 to 4.6 mg/L; Supplementary Material SM3). These values are higher than those commonly observed in other AMD environments (generally tens to hundreds of µg/L according to Migaszewski and Galuszka, 2005). The amount of ΣREE transport by the first four AMD sources to the Odiel River ranged from 31 g/day (Esperanza) to 331 g/day (Poderosa) while the load delivered by the Agrio River was significantly higher (16.4 kg/day).

4.2. Physico-chemical parameters and elements concentrations along the river reach

Autumn rainfalls occurring before the sampling were relatively low (75 mm). As a consequence, the river flow exhibits intermediate to low values, from 296 L/s at sampling point O1 to 343 L/s at O8 (Supplementary Material SM1). Above the confluence of the first AMD source, pH and EC values were 8.01 and 0.28 mS/cm (point O1), respectively, with a total alkalinity of 81 mg/L $CaCO_3$. Along the river reach covering points O2 to O7 (Fig. 1), pH values ranged from 7.0 to 7.7 despite the confluence of several AMD inputs, while EC values increased progressively from 0.30 to 0.34 mS/cm and alkalinity decreased down to 66 mg/L $CaCO_3$ (Supplementary Material SM1). A drastic change in the hydrochemical characteristics of the river is observed at point O8 beyond the confluence of the strongly acidic and metal-rich waters of the Agrio River, with a decrease in the pH value down to 2.98 and an increase in EC up to 2.26 mS/cm. Downstream, these conditions continued with slight variations until the river mouth into the estuary was reached (Sarmiento et al., 2009).

Sulphate and metal concentrations exhibit low values in the dissolved (8.4 mg/L sulphate and below 3 µg/L for As, Cu, Co, Zn, etc.) and total samples (< 10 µg/L for the latter trace metals) upstream of the confluence with the first AMD input (point O1). Then, as a consequence of the AMD inputs, the sulphate concentration progressively increases up to a value of 72 mg/L at O7, which is subsequently increased to 2061 mg/L below the confluence with the Agrio River. The dissolved concentrations of Fe and Al remain relatively low (< 0.3 mg/L) along the river up to point O7 (Fig. 2) because there is intense precipitation of these elements when the AMD inputs are neutralized by mixing with circumneutral river water (Cánovas et al., 2018). Thus, the transport of these elements primarily takes place in the particulate matter, and the total concentrations (up to 5.4 mg/L Fe and 1.6 mg/L Al) are much higher than the dissolved concentrations. During the mixing of the Agrio and Odiel river waters, intense precipitation of Fe is observed, as demonstrated by the higher concentrations of total Fe (41 mg/L) compared to dissolved Fe (27 mg/L; Supplementary Material, SM2). On the other hand, total and dissolved Al concentrations are similar (Fig. 3; Supplementary Material SM2).

In the case of Mn and to a lesser extent Zn, total and dissolved concentrations are approximately similar along the reach (Fig. 2); thus, transport takes place mainly in the dissolved phase. Analogous behaviour is observed for Cd, Co, and Ni (Supplementary Material SM4). The evolution of As, Cu, and Pb along the river reach shows a different behaviour, with a greater significance of particulate transport (Fig. 2).

Dissolved concentrations of ΣREE increase from 0.07 µg/L at O1 to 0.16-1.82 µg/L between points O2 and O7. These values are similar to those found in other rivers worldwide, ranging from ng/L to tens of µg/L (Elderfield et al., 1990; Leybourne and Johannesson, 2008; Migaszewski and Galuszka, 2015). At O8 sampling point the confluence of the Agrio River, which carries acidic and metal-rich waters from the Río Tinto mines (Cánovas et al., 2018), causes a pH decrease below 3. In these conditions REE behave conservatively, reaching a dissolved concentration of 553 µg/L. This value, several orders of magnitude higher than those found in natural waters, are common in the AMD-affected waters of the IPB (Ferreira da Silva et al., 2009; Ayora et al., 2016) and other acidic streams worldwide (e.g. Gammons et al., 2005; Migaszewski and Galuszka, 2015). On the other hand, total concentrations of ΣREE are relatively low upstream the confluence with the first AMD input (0.52 µg/L, point O1) but undergo a sharp increase until point O5 (25 µg/L). Downstream of this point, there is a reach of around 4 km in length (Fig. 1) with an absence of AMD sources where dissolved and total ΣREE concentrations decrease, as for other elements (Fig. 2). Below the confluence with the Agrio River almost 100% of the ΣREE is transported in the dissolved phase (Fig. 2).

4.3. REE NASC-normalized patterns

All AMD sources are characterized by exhibiting NASC-normalized patterns with an enriched MREE signature (Fig. 3), which is commonly found in this type of water (e.g., Gimeno-Serrano et al., 2000; Verplanck et al., 2004; Ayora et al., 2016). However, some differences can be appreciated. The Agrio River shows the highest value of Ce* (1.21, whereas the rest of the AMD sources range from 0.99 to 1.03) and Eu* (0.89, whereas the rest range from 0.63 to 0.83; SM3). The AMD from San Platón stands out by its low HREE content (low values of $(MREE/LREE)_N$ and $(HREE/MREE)_N$ ratios). Poderosa also shows a pattern with a depleted HREE signature in relation to MREE, although to a lesser extent than San Platón, and the lowest negative Eu* (0.63). Concepción stands out by showing a relatively flat pattern, even though there is a slight HREE depletion. Esperanza exhibits a similar pattern to that of the Agrio River (Fig. 3), although with the lowest value of Ce* (1.00). The NASC-normalized patterns of the AMD sources remained constant throughout the year despite the seasonal variations in REE concentrations related mainly to dilution processes during rainy periods (Olías et al., 2017).

The REE signature of the AMD inputs influences the NASC-normalized pattern of the total concentrations along the sampling points in the river (Figs. 3 and 4). However, the dissolved concentrations show different patterns. An interesting observation is the $(HREE/MREE)_N$ enrichment in the dissolved samples with respect to the total samples along the reach (Fig. 4B). Also, the confluence of the first AMD input causes an increase in Ce* in the river in both the

dissolved and, above all, total concentrations (Fig. 4C). Values of Ce* in the total concentrations are generally higher than in the dissolved along the river reach. The opposite tendency is observed for Eu*; a decrease is observed in both dissolved and total concentrations along the reach as a consequence of the AMD inputs except at O3, which suggests the existence of not sampled acidic diffuse inputs. In the reach between points O6 and O7, characterized by the absence of AMD inputs, a decrease in Ce* in dissolved samples is observed whereas Eu* increases (Fig. 4C and D).

4.4. REE speciation

The chemical speciation of REE shows that carbonate complexes ($REE(CO_3)^+$ and $REE(CO_3)_2^-$) predominate between O1 and O7. However, sulphate complexes ($REE(SO_4)^+$) prevail at O8, where acid pH values and higher sulphate concentrations are observed. On the other hand, some differences can be appreciated between individual REE (Fig. 5). Thus, the carbonate complexes for the HREE (represented by Yb) constitute more than 95% of the total up to O7, while lower values (from 59 to 98%) are observed for LREE (represented by La) in favour of free forms and sulphate complexes (Fig. 5). A growing increment in the proportion of these latter species is observed concomitant with the progressive increase of sulphate concentrations along the river reach. However, some fluctuations in this evolution are observed due to pH changes that control the CO_3^{2-} concentration and, thus, the significance of carbonate complexes. On the other hand, Gd shows an intermediate behaviour, with a lower percentage of carbonate complexes with respect to Yb and a lower percentage of sulphate complexes and free forms than La (Fig. 5).

5. DISCUSSION

5.1. REE concentrations along the river reach

Figure 6 shows a clear inverse relationship between dissolved ΣREE concentrations and pH. This relation has been previously reported in other rivers both affected by AMD (Verplanck et al., 2004; Sun et al., 2012; Stewart et al., 2017) and not affected (e.g., Elderfield et al., 1995; Xu and Han, 2009). Total ΣREE concentrations are much higher than dissolved concentrations at pH values above 7; thus, the transport of ΣREE along the river is mainly carried out by particulate matter (70 to 97% of the total). This situation is reversed at pH below 3 due to the acidity limiting surface adsorption processes onto the particulate matter (Sholkovitz, 1995), and thus, almost 100% of ΣREE transport is carried out by the dissolved phase (Fig. 2). It can be calculated that the sum of the ΣREE loads at points O6 and O7 is similar to the load at point O8, despite intense Fe precipitation. This fact is in agreement with Verplanck et al. (2004), who reported a conservative behaviour of ΣREE below pH 5.1 and REE sorption/coprecipitation at pH values between 5.1 and 6.1, and with Gammons et al. (2005), who observed REE removal when pH increased from 4.3 to 6.1. Ferreira da Silva et al. (2009) and Prudencio et al. (2015) also reported that REE were removed from solution during pH increases from 3 to 6. More recently, Ayora et al. (2016) found preferential removal of REE with Al precipitates (above pH 4.5) during AMD treatment. In this sense, Figure 7 shows that the percentage of dissolved REE (represented by La) in samples

collected along the river follows a similar evolution to that of Al. This seems to indicate REE removal due to the coprecipitation with this element, as previously observed by Gammons et al. (2005) and Ayora et al. (2016).

A decrease in the percentage of dissolved ΣREE is observed from points O1 to O5, despite a slight decrease in the pH values, due to the increase in particulate concentration by sorption/coprecipitation of REE during the neutralization of the AMD inputs by the river water (Fig. 2). Downstream of O6, the dissolved percentage increases (Fig. 7) due to the decrease of particulate matter by sedimentation.

5.2. REE fractionation processes along the river reach

As shown in section 4.3, the NASC-normalized patterns of total concentrations along the river reach vary influenced by the pattern of the different AMD inputs (Figs. 3 and 4), whereas the dissolved NASC-normalized patterns are also affected by in-stream processes. This can be clearly seen from the differences in the NASC-normalized patterns between points O6 and O7, which is a long subreach without any AMD input (Fig. 1). The NASC-normalized patterns for total samples (Figs. 3 and 4) are similar at both points, although the concentrations are much lower at O7 due to sedimentation processes. On the contrary, the patterns for the dissolved concentrations show clear differences (Figs. 3 and 4).

Figure 8 shows that, in general, the lowest dissolved percentages are observed for LREE (except for La and, to a lesser extent, Ce) and MREE whereas the highest are found for HREE. For the HREE, our data apparently disagree with results previously obtained by other authors (e.g., Verplanck et al., 2004; Liu et al., 2017), who reported preferential removal of HREE from solution during Fe oxyhydroxide precipitation while LREE, especially La, tend to remain dissolved. However, the pH values of Verplanck et al. (2004) are lower than 6.2 whereas in the Odiel River, with pH between 7 and 8 upstream of the Agrio River, the formation of carbonate complexes with HREE (Fig. 5) must have a greater influence, and therefore it counteracts the preferential removal of HREE by oxyhydroxide precipitates. In this sense, Leybourne et al. (2000) and Johannesson and Lyons (1994) reported preferential REE complexation by carbonate in water as well as LREE-depleted NASC-normalized REE patterns and higher enrichment in HREE than in MREE. A similar conclusion was obtained by Sholkovitz (1995) who showed that suspended and colloidal particles in river water are typically LREE-enriched compared to NASC with preferential loss from solution by adsorption following the order LREE > MREE > HREE. In brief, Ce and particularly La have higher dissolved percentages (Fig. 8) because they are less intensely sorbed by Fe oxyhydroxides while HREE also have high dissolved percentages because of the preferential formation of carbonate complexes. Both processes lead to fractionation of REE between dissolved and solid phases.

On the other hand, as noted in section 4.3, Ce* tends to be higher in total samples while the opposite is observed for Eu* (Fig. 4C and D). In the case of Ce*, the high oxidizing capacity of Fe oxyhydroxide-precipitating systems may enhance the oxidation of Ce(III) and its partition into the solid phase (Bau, 1999). However, speciation results provided by CHEAQS show that Ce (and also

Eu) is found in its trivalent form, and these differences cannot be explained by different oxidation states. Instead, this seems to be related to the higher tendency of La to remain dissolved, which decreases the anomaly value. Thus, a remarkable decrease of the negative Ce* in the dissolved phase takes place between O6 and O7 (Fig. 4C), despite the absence of any AMD inputs. Between these points the dissolved and total concentrations of La, Ce, and Nd decrease, but not to the same degree. The dissolved concentration of La decreases by 72% with respect to the value at O6 (Fig. 9) while Ce decreases 81% and Nd 83%, which explains the decrease in the Ce* value. On the contrary, total concentrations of La, Ce, and Nd decrease by a similar percentage (77-78%) between points O6 and O7; thus, there are no differences in Ce* (Fig. 4C). In the same way, the variations in Eu* between the total and dissolved phases could also be due to slight hydrogeochemical differences between Sm, Eu, and Gd.

5.3. Possible ecotoxicity of REE

High concentrations of REE could lead to ecotoxicity problems such as disruption of bone-integrity and cellular signalling by competition between La and Ca or Mg, substitution of Fe by Sc, lipid-peroxidation and phosphate deficiency (Gonzalez et al., 2014). The toxicity of REE depends on several factors such as the exposure method, the life stage of the organism and the nature and concentration of the REE (Gwenzi et al., 2018). In this way, insoluble forms of lanthanides have shown low toxicity, while higher toxicity was reported for soluble compounds (Lambert and Ledrich, 2014). On the other hand, an increase in toxicity has been considered with increasing REE atomic number, thus HREE have been usually predicted to be more toxic than LREE (Gonzalez et al., 2014). However, REE ecotoxicological experiments found in literature provides contradictory results due to the lack of information on REE chemical speciation, the formation of insoluble species during the tests and the existence of other compounds that may pose a toxicity risk for living organisms (Gonzalez et al., 2014).

AMD formation leads to the release of significant quantities of REE into the watercourses, however, in circumneutral waters like those found in the studied reach, a predominant transference from the dissolved to the particulate phase takes place, limiting the ecotoxicity risk. On the other hand, despite the low content in HREE compared to LREE in AMD waters, the complexation of HREE by carbonates in circumneutral waters favours its solubility, thus increasing their toxicity. From the study of mollusc communities in the Odiel River Pérez-Quintero (2011) reported a good ecological quality status upstream of the first AMD input (sampling point O1) while turned to poor between points O2 to O7. Downstream of the Agrio River confluence, with pH values close to 3, the natural river communities completely disappear. The role of the REE concentrations in these ecological effects is not clear because of the presence of other trace metal/loids in the water such as Al, As, Cd, etc. (Supplementary Material SM2), which must contribute to the ecotoxicity problems, masking the influence of REE as indicated by Gonzalez et al. (2014).

6. CONCLUSIONS

The studied river reach receives several AMD inputs; however, upstream of the Agrio River the higher river streamflow and water alkalinity is enough to maintain pH values above 7. This causes the precipitation of dissolved Fe and Al delivered by the AMD sources, leading to the occurrence of large amounts of particulate matter.

AMD sources also carry high quantities of ΣREE to the Odiel River, i.e., 16.4 kg/day from the Agrio River. However, whereas pH values remain above 7, dissolved ΣREE concentrations stay relatively low (< 1.8 μg/L) and ΣREE transport takes place mainly in the particulate matter (between 70 and 97% of the total). On the contrary, the transport of other trace elements such as Cd, Co, Ni, Mn, and Zn is mainly carried out by the dissolved phase. When pH values decrease down to 3, REE behave conservatively in the river, and transport is performed in the dissolved phase. Due to the existence of significant concentrations of other metal/loids in these systems, the ecotoxicological effects of the REE is not clear and should be the subject of further investigations.

The NASC-normalized REE patterns of total concentrations in the river accurately resemble that of the corresponding AMD sources, and in the absence of further AMD inputs, remain invariable. However, the total REE concentration decreases as a result of sedimentation processes. On the other hand, the NASC-normalized patterns of dissolved REE in the river are strongly affected by the AMD inputs but deviate from them due to 1) the tendency of LREE, especially La, to remain dissolved during Fe oxyhydroxide precipitation and more importantly 2) HREE complexation by carbonates, which favours its permanence in solution. This process is clearly evident in the longest subreach, between points O6 and O7, where fractionation processes occur despite the absence of further AMD inputs.

Variations in the Ce and Eu anomalies are observed along the river reach as a consequence of the different AMD inputs. Nevertheless, there are striking differences between the dissolved and particulate phases. The values of Ce* are slightly higher in total samples than in dissolved samples, whereas the opposite is observed for Eu*. Speciation results seem to indicate that this is not caused by differences in oxidation states but by slight differences in the Ce hydrogeochemical behaviour with respect La and Nd. In this way, due to the higher affinity of La for remaining dissolved in relation to Ce and Nd, a slight decrease in Ce* is produced in the dissolved phase. In the same way, small differences in the behaviour of Eu with respect to Sm and Gd can also cause variations in Eu* between the dissolved and particulate phases.

Acknowledgements

This work was funded by the CGL2013-48460-C2-1-R, CGL2016-78783-C2-1-R, LIFE-ETAD ENV/ES/000250 and ERAMIN PCIN-2015-242-256 projects. M.D. Basallote also thanks the Spanish Ministry of Economy and Competitiveness for the Postdoctoral Fellowship granted under application references FJCI-2015-24765. C.R Cánovas was funded by the Talent Consolidation Program of the University of Huelva. The authors would like to thank the helpful comments of the

Editor-in-Chief Karen Johannesson and two anonymous reviewers that notably improved the quality of the manuscript.

References

Ayora, C., Macías, F., Torres, E., Lozano, A., Carrero, S., Nieto, J.M., Pérez-López, R., Fernández-Martínez, A., Castillo Michel, H.. 2016. Recovery of Rare Earth Elements and Ytrium from passive remediation systems of acid mine drainage. Environ. Sci. Technol. 50, 8255-8262.

Bau, M., 1999. Scavenging of dissolved yttrium and rare earths by precipitating iron oxyhydroxide: experimental evidence for Ce oxidation, Y-Ho fractionation, and lanthanide tetrad effect. Geochim. Cosmochim. Acta 63, 67–77.

Cánovas, C.R., Riera, J., Carrero, S., Olías, M., 2018. Dissolved and particulate metal fluxes in an AMD affected stream under different hydrological conditions: The Odiel River (SW Spain). Catena 165, 414-424.

Carrera, J., Vázquez-Suñé, E., Castillo, O., Sánchez-Vila, X., 2004. A methodology to compute mixing ratios with uncertain end-members. Water Resour. Res. 40, W12101.

Dia, A., Gruau, G., Olivié-Lauquet, G., Riou, C., Molénat, J., Curmi, P., 2000. The distribution of rare earth elements in groundwaters: Assessing the role of source-rock composition, redox changes and colloidal particles. Geochim. Cosmochim. Acta 64, 4131-4151.

Elderfield, H., Upstill-Goddard, R., Sholkovitz. E.R., 1990. The rare earth elements in rivers, estuaries and coastal sea waters: Processes affecting crustal input of elementos to the ocean and their significance to the composition of seawater. Geochem. Cosmochim. Acta 54, 971-991.

Ferreira da Silva, E., Bobos, I., Matos, J.X., Patinha, C., Reis, A.P., Cardoso Fonseca, E., 2009. Mineralogy and geochemistry of trace metals and REE in volcanic massive sulfide host rocks, stream sediments, stream waters and acid mine drainage from the Lousal mine area (Iberian Pyrite Belt, Portugal). Appl. Geochem. 24, 383-401.

Galván, L., Olías, M., Cánovas, C.R., Sarmiento, A.M., Nieto, J.M., 2016. Hydrological modeling of a watershed affected by acid mine drainage (Odiel River, SW Spain). Assessment of the pollutant contributing areas. J. Hydrol. 540, 196–206.

Gammons, C.H., Wood, S.A., Pedrozo, F., Varekamp, J.C., Nelson, B.J., Shope, C.L., Baffico G. , 2005. Hydrogeochemistry and rare earth element behavior in a volcanically acidified watershed in Patagonia, Argentina. Chem. Geol. 222, 249–267.

Gimeno Serrano, M.J., Sanz, L.F.A., Nordstrom, D.K., 2000. REE speciation in low-temperature acidic waters and the competitive effects of aluminum. Chem. Geol. 165, 167–180.

Gonzalez, V., Vignati, D.A.L., Leyval, C., Giamberini, L., 2014. Environmental fate and ecotoxicity of lanthanides: are they a uniform group beyond chemistry?. Environ. Int. 71, 148–157.

Grawunder, A., Merten, D., Büchel, G., 2014. Origin of middle rare earth element enrichment in acid mine drainage impacted areas. Environ. Sci. Pollut. Res. 21, 6812–6823.

Gwenzi,W., Mangori, L., Danha, C., Chaukura, N., Dunjana, N., Sanganyado, E., 2018. Sources, behaviour, and environmental and human health risks of high-technology rare earth elements as emerging contaminants. Sci. Total Environ. 636, 299-313.

Hatch, G.P., 2012. Dynamics in the Global Market for Rare Earths. Elements 8, 341–346.

Huang, X.C., Zhang, G., Pan, A.F., Chen, F., Zheng, C., 2016. Protecting the environment and public health from rare earth mining. Earth's Future 4, 532-535.

Johannesson, K. H., Lyons, W. B., 1994. The rare earth element geochemistry of Mono Lake water and the importance of carbonate complexing. Limnol. Oceanogr. 39, 1141–1154.

Johannesson, K.H., Stetzenbach, K.J., Hodge, V.F., 1997. Rare earth elements as geochemical tracers of regional groundwater mixing. Geochim. Cosmochim. Acta 61, 3605-3618.

Kulaksiz, S., Bau, M., 2007. Contrasting behaviour of anthropogenic gadolinium and natural rare earth elements in estuaries and the gadolimnium imput into the North Sea. Earth Planet. Sci. Lett. 260, 361-371.

Kurvet, I., Juganson, K., Vija, H., Sihtmäe, M., Blinova, I., Syvertsen-Wiig, J., Kahru, A., 2017. Toxicity of Nine (Doped) Rare Earth Metal Oxides and Respective Individual Metals to Aquatic Microorganisms Vibrio fischeri and Tetrahymena thermophile. Materials 10: 754.

Lambert, C.E., Ledrich, M.L., 2014. Lanthanide series of metals. Encyclopedia of Toxicology (third edition), vol. 3, pp. 43-47

Leybourne, M.I., Goodfellow, W.D., Boyle D.R., Hall G.M., 2000. Rapid development of negative Ce anomalies in surface waters and contrasting REE patterns in groundwaters associated with Zn–Pb massive sulphide deposits. Appl. Geochem. 15, 695–723.

Leybourne, M.I., Johannesson, K.H., 2008. Rare earth elements (REE) and yttrium in stream waters, stream sediments and Fe-Mn oxyhydroxides: Fractionation, speciation and controls over REE+Y patterns in the surface environments. Geochim. Cosmochim. Acta 72, 5962-5983.

Liu, H., Pourret, O, Guo, H, Bonhoure, J., 2017. Rare earth elements sorption to iron oxyhydroxide: Model development and application to groundwater. Appl. Geochem. 87, 158–166.

Migaszewski, Z.M., Galuszka, A., 2015. The characteristics, occurrence, and geochemical behavior or rare earth elements in the environment: a review. Crit. Rev. Environm. Sci. Technol. 45, 429-471.

Nieto, J.M., Sarmiento, A.M., Cánovas, C.R., Olías, M., Ayora, C., 2013. Acid mine drainage in the Iberian Pyrite Belt: 1. Hydrochemical characteristics and pollutant load of the Tinto and Odiel Rivers. Environ. Sci. Pollut. Res. 20, 7509-7519.

NIST, 2004. NIST Standard Reference Database 46 Version 8.0, A.E. Martell & R.M. Smith (eds.), Gaithersburg, USA.

Nordstrom, D.K., Wilde, F.D., 1998. Reduction–oxidation potential (electrode method), in: National Field Manual for the Collection of Water Quality Data, Book 9, Chapter 6.5. U.S. Geological Survey Techniques of Water-Resources Investigations, Reston, VA, pp. 1-22.

Nordstrom, D.K., Bowell, R.J., Campbell, K.M., Alpers, C.N., 2017. Challenges in recovering resources from acid mine drainage, in: Wolkersdofer, C., Sartz, L. Sillanpää, M., Häkinnen, A. (Eds), Proceedings of 13th International Mine Water Association Congress, Lapperanta, Finland, vol. 2 pp. 1138-1146.

Olías, M., Nieto, J.M., 2015. Background conditions and mining pollution throughout history in the Río Tinto (SW Spain). Environments 2, 295–316.

Olías, M., Cánovas, C.R., Riera J., 2017. Temporal variations of REE in several AMD sources of the Odiel River (SW Spain). Procedia Earth Planet. Sci. 17, 707-709.

Pérez-López, R., Nieto, J.M., De la Rosa, J., Bolívar, J.P., 2015. Environmental tracers for elucidating the weathering process in a phosphogypsum disposal site: implications for restoration. J. Hydrol. 559, 1313-1323.

Pérez-Quintero, M.A., 2011. Freshwater mollusc biodiversity and conservation in two stressed Mediterranean basins. Limnologica 41, 201–212.

Pinedo Vara, I., 1963. Piritas de Huelva Su historia, minería y aprovechamiento, Summa, Madrid.

Prudencio, M.I., Valente, T., Marques, R., Sequeira Braga, M.A., Pamplona, J., 2015. Geochemistry of rare earth elements in a passive treatment system built for acid mine drainage remediation. Chemosphere 138, 691-700.

Sánchez España, J., López Pamo, D., Santofimia Pastor, E., Reyes Andrés, J., Martín Rubí, J.A., 2006. The impact of acid mine drainage on the water quality of the Odiel River (Huelva, Spain). Evolution of precipitate mineralogy and aqueous geochemistry along the Concepcion-Tintillo segment. Water Air Soil Pollut. 173, 121-149.

Sáez, R., Pascual, E., Toscano, M., Almodóvar, G.R., 1999. The Iberian type of volcanosedimentary massive sulphide deposits. Miner. Deposita 34, 549–570.

Sarmiento, A.M., Nieto, J.M., Olías, M., Cánovas, C.R., 2009. Hydrochemical characteristics and seasonal influence on the pollution by acid mine drainage in the Odiel River basin (SW Spain). Appl. Geochem. 24, 697-714.

Sholkovitz E.R., 1995. The aquatic chemistry of Rare Earth Elements in Rivers and Estuaries. Aquatic Geochem. 1, 1-34.

Stewart, B.W., Capo, R.C, Hedin, B.C, Hedin, R.S., 2017. Rare earth element resources in coal mine drainage and treatment precipitates in the Appalachian Basin, USA. Int. J. Coal Geol. 169, 28–39.

Stille, P., Gauthier-Lafaye, F., Jensen, K.A., Salah, S., Bracke, G., Ewing, R.C., Louvat, D., Million, D., 2003. REE mobility in groundwater proximate to the natural fission reactor at Banbombé (Gabon). Chem. Geol. 198, 289-304.

Stolpe, B., Guo, L., Shiller, A.M., 2013. Binding and transport of rare earth elements by organic and iron-rich nanocolloids in Alaskan rivers, as revealed by field-flow fractionation and ICP-MS. Geochim. Cosmochim. Acta 106, 446–462.

Sun, H, Zhao, F., Zhang, M., Li, J., 2012. Behavior of rare earth elements in acid coal mine drainage in Shanxi Province, China. Environ. Earth. Sci. 67, 205–213.

Taylor, S.R., McLennan, S.M., 1985. The continental crust: its composition and evolution, Blackwell Scientific Publications, Oxford.

Tornos, F., 2006. Environment of formation and styles of volcanogenic massive sulfides: The Iberian Pyrite Belt. Ore Geol. Rev. 28, 259–307.

Verplanck, P.L., Nordstrom, D.K., Taylor, H.E., 1999. Overview of rare earth element investigations in acid water or U.S. Geological Survey abandoned mine land watersheds, in: Contamination from hard rock mining, Water Resources Investigation Report 99-4018A, pp. 83-92.

Verplanck, P.L., Nordstrom, D.K., Taylor, H.E., Kimball, B.A., 2004. Rare earth element partitioning between hydrous ferric oxides and acid mine water during iron oxidation. Appl. Geochem. 19, 1339-1354.

Verweij, W., 2017. Manual for CHEAQS Next, a program for calculating Chemical Equilibria in Aquatic Systems.

Worrall, F., Pearson, D.G., 2001. Water-rock interaction in an acidic mine discharge as indicated by rare earth element patterns. Geochim. Cosmochim. Acta 65, 3027-3040.

Xu, Z., Han, G., 2009. Rare earth elements (REE) of dissolved and suspended loads in the Xijiang River, South China. Appl. Geochem 24, 1803–1816.

List of figures

Supplementary Material

SM4. Total and dissolved concentrations along the river reach (sampling points O1 to O8, blue lines) and inputs from AMD sources (red vertical bars) of trace elements not represented in Figure 2. Dissolved and total inputs of AMD sources are similar.

Figure 1

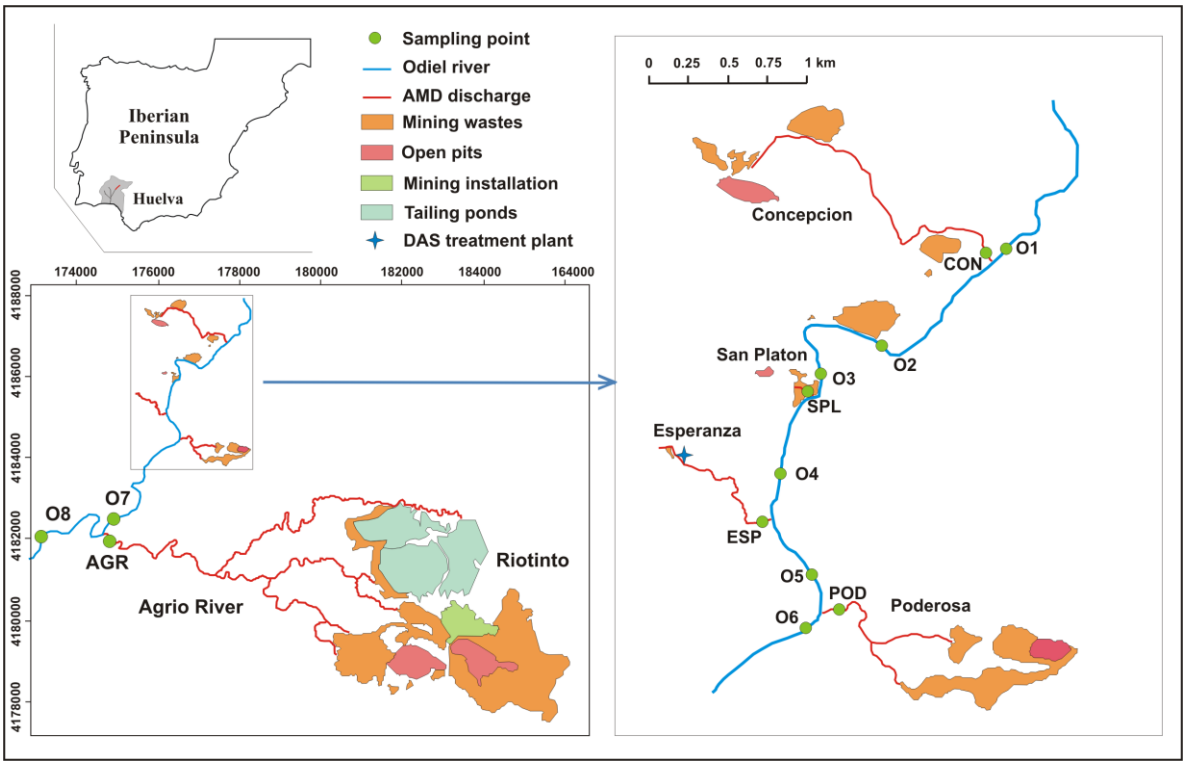
Iberian Peninsula
Huelva
Sampling point
Odiel river
AMD discharge
Mining wastes
Open pits
Mining installation
Tailing ponds
DAS treatment plant
174000
176000
178000
180000
182000
184000
164000
4188000
4186000
4184000
4182000
4180000
4178000
O8
O7
AGR
Agrio River
Riotinto
0 0.25 0.5 0.75 1 km
Concepcion
CON
O1
O2
San Platon
O3
SPL
Esperanza
O4
ESP
O5
POD
O6
Poderosa

Figure 2

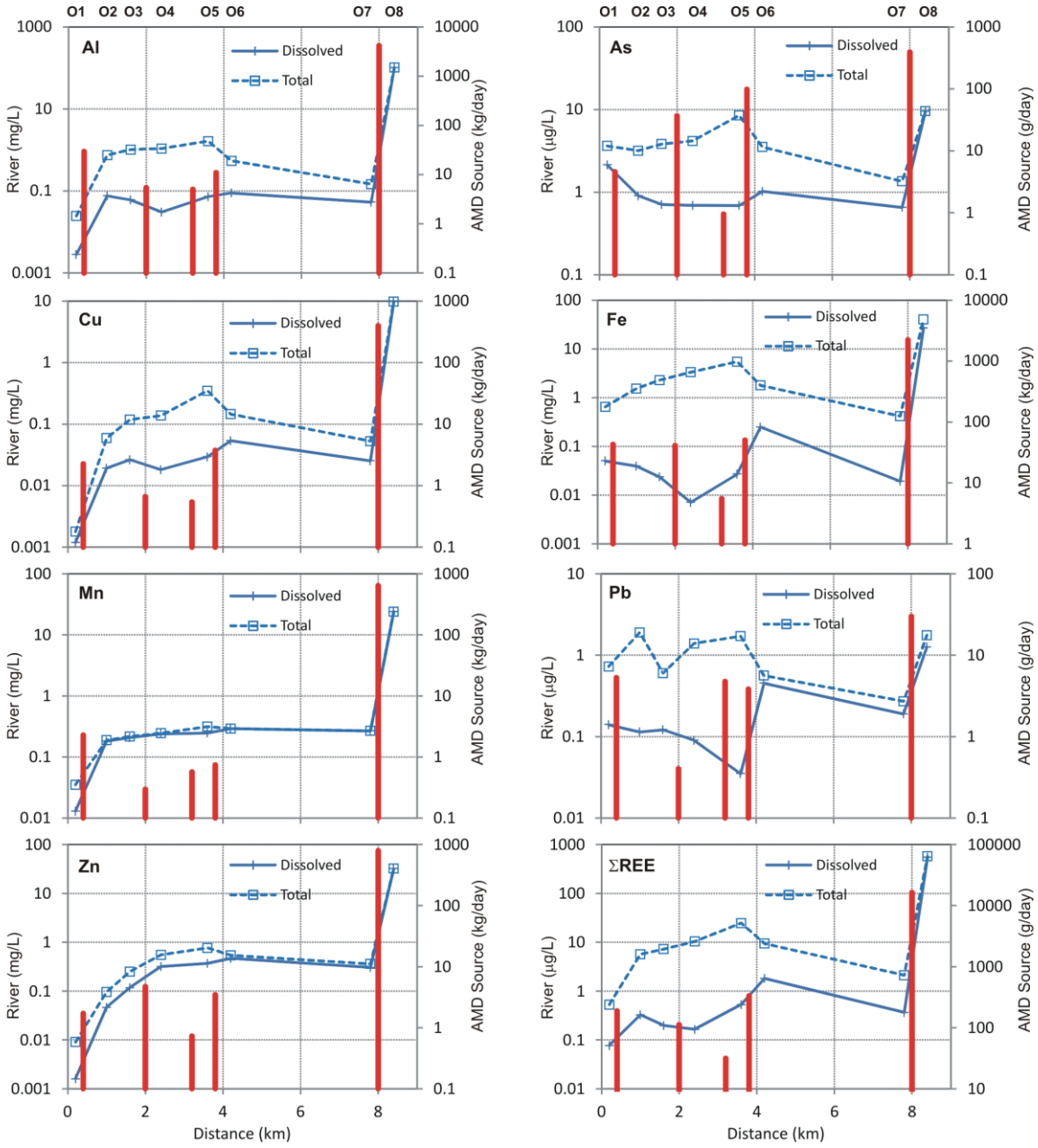
O1 O2 O3 O4 O5 O6 O7 O8
Al
As
Cu
Fe
Mn
Pb
Zn
ΣREE
Dissolved
Total
River (mg/L)
River (µg/L)
AMD Source (kg/day)
AMD Source (g/day)
Distance (km)

Figure 3

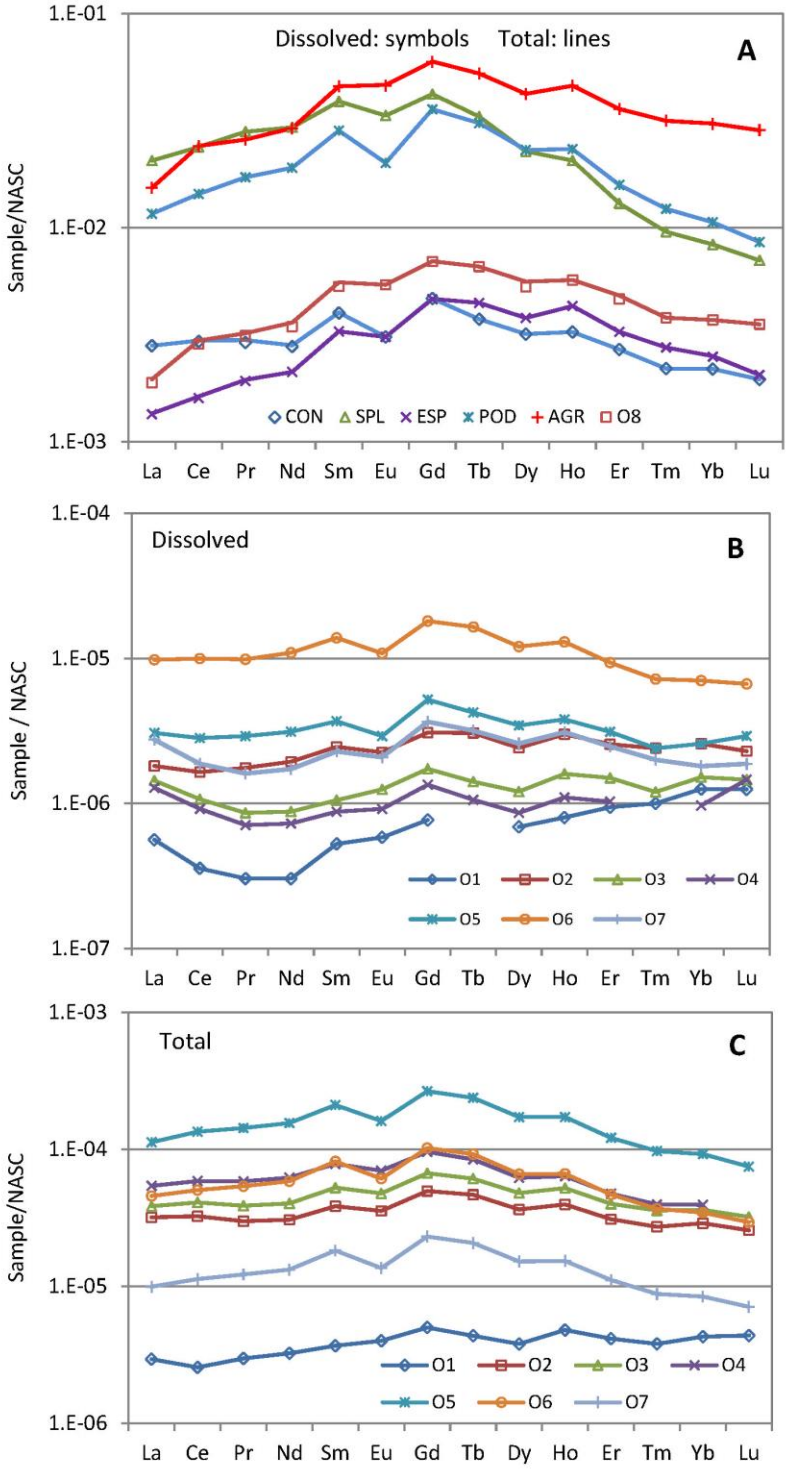
Dissolved: symbols Total: lines
A
Sample/NASC
1.E-01
1.E-02
1.E-03
CON SPL ESP POD AGR O8
La Ce Pr Nd Sm Eu Gd Tb Dy Ho Er Tm Yb Lu
Dissolved
B
Sample / NASC
1.E-04
1.E-05
1.E-06
1.E-07
O1 O2 O3 O4
O5 O6 O7
La Ce Pr Nd Sm Eu Gd Tb Dy Ho Er Tm Yb Lu
Total
C
Sample/NASC
1.E-03
1.E-04
1.E-05
1.E-06
O1 O2 O3 O4
O5 O6 O7
La Ce Pr Nd Sm Eu Gd Tb Dy Ho Er Tm Yb Lu

Figure 4

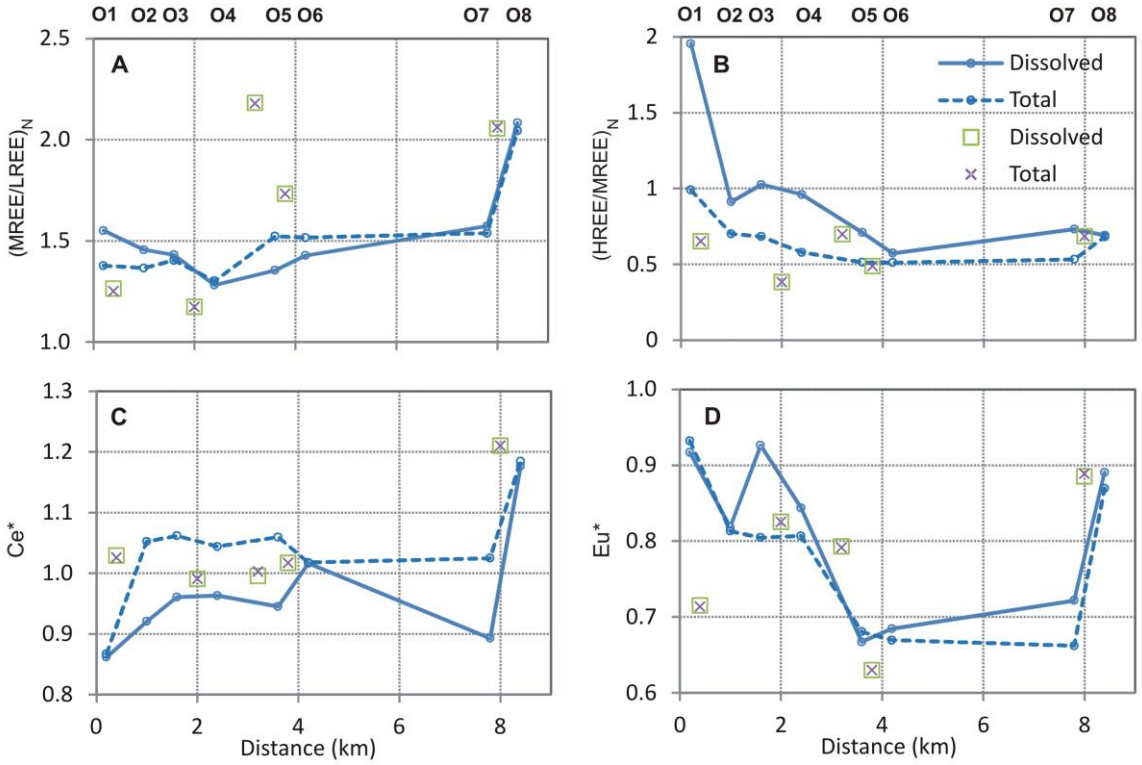

Figure 5

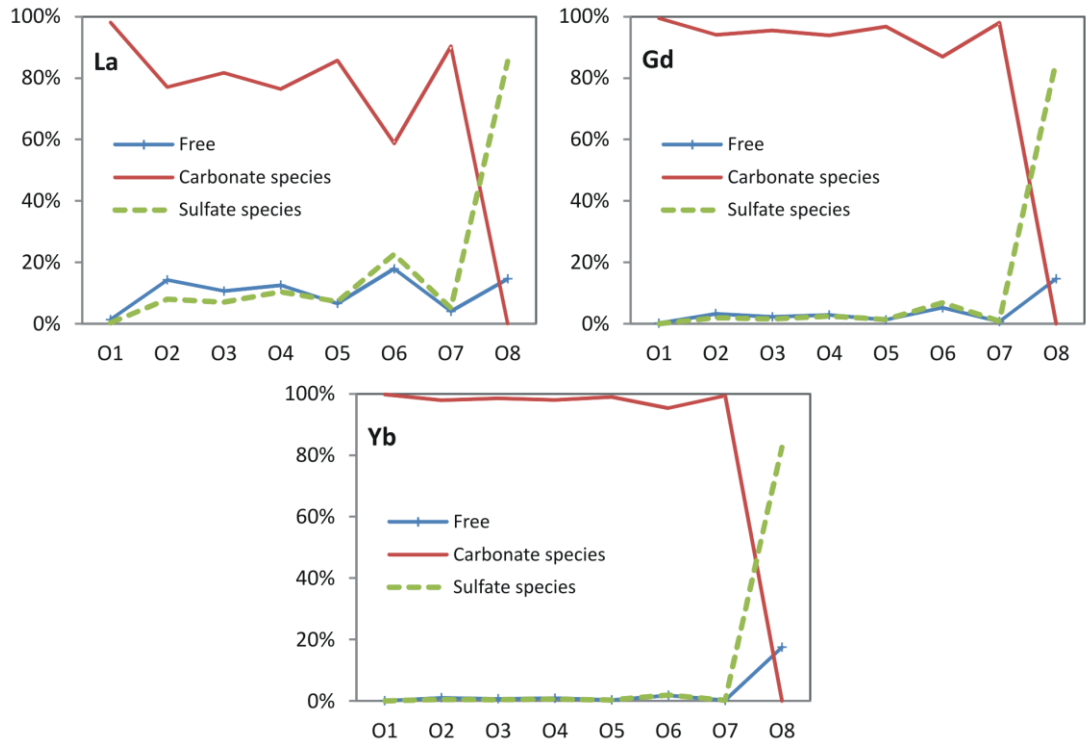

Figure 6

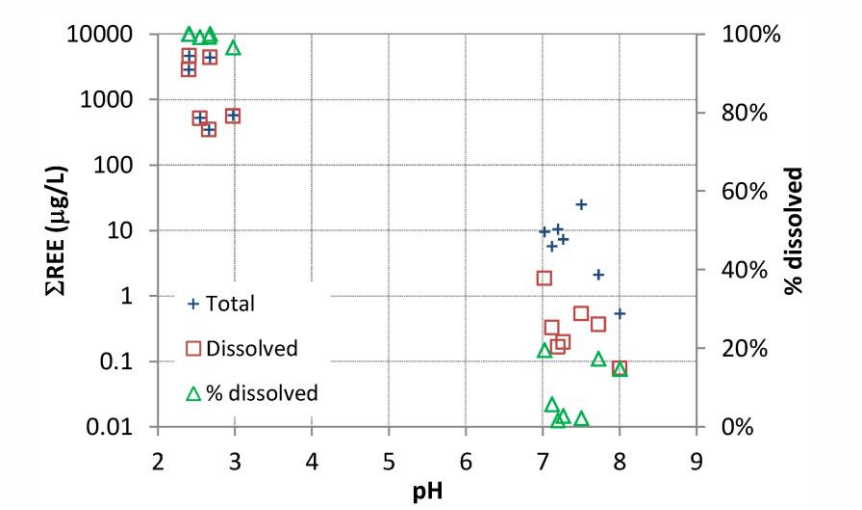

Figure 7

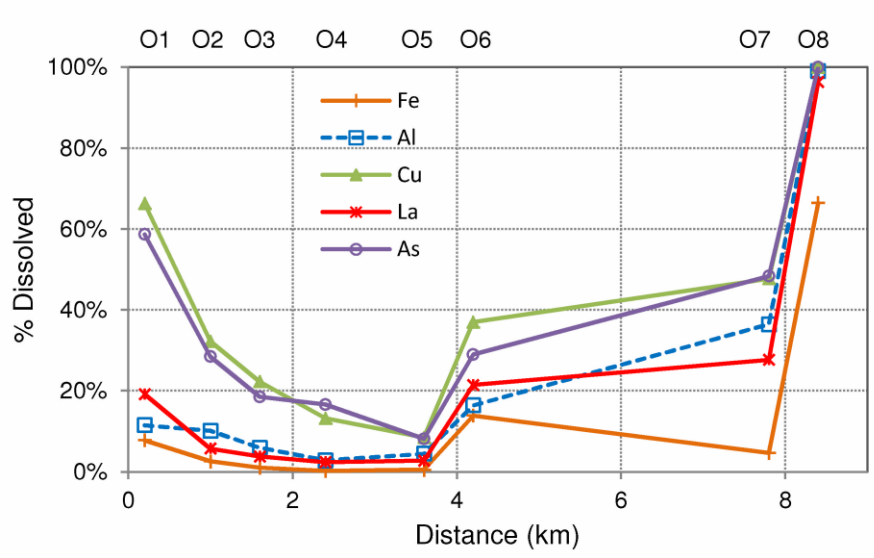

Figure 8

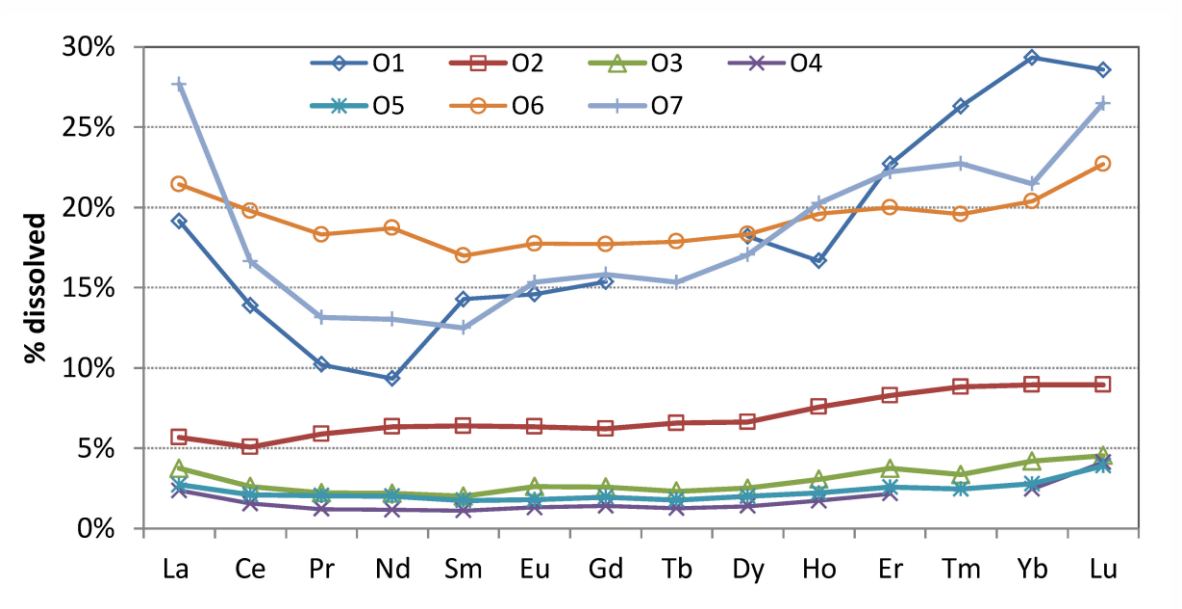

Figure 9